Available online at www.sciencedirect.com
ScienceDirect
Precambrian Research 151 (2006) 101–118
Precambrian Research
www.elsevier.com/locate/precamres

The mafic layered complex of the Kabyé massif (north Togo and north Benin): Evidence of a Pan-African granulitic continental arc root

G. Duclaux [a,b,*], R.P. Ménot [a], S. Guillot [c], Y. Agbossoumondé [d], N. Hilairet [e]

[a] Laboratoire de Transferts Lithosphériques, CNRS-UMR 6524, Magmas et Volcans, Université Jean Monnet, 23 rue Dr. P. Michelon, 42023 Saint Étienne Cedex 2, France
[b] EarthByte Group, School of Geosciences, The University of Sydney, NSW 2006, Australia
[c] Laboratoire de Géodynamique des Chaînes Alpines, CNRS-UMR 5025, Université Joseph Fourier, 1381, rue de la Piscine, 38400 Saint Martin d'Hères, France
[d] Département des Sciences de la Terre, Université de Lomé, B.P. 1515 Lomé, Togo
[e] Laboratoire des Sciences de la Terre, CNRS-UMR 5570, École Normale Supérieure de Lyon, 46 Allée d'Italie, 69364 Lyon Cedex 7, France

Received 2 March 2006; received in revised form 28 July 2006; accepted 26 August 2006

Abstract

Between the predominantly Neoarchean–Paleoproterozoic West African Craton (WAC) and the Saharian Metacraton (SMC), the Dahomeyides suture zone represents a valuable witness of continental amalgamation during Pan-African times. In the Kabyé massif (northern Togo and northern Bénin) mainly granulitic metagabbros, associated with Al-rich kyanite and garnet bearing felsic dykes, are exposed as tectonic lenses within the pre-Pan-African gneisses of the SMC. New geochemical data suggest that the high grade rocks (granulites) in the Kabyé massif originated in a mature continental arc setting. AFC calculations constrain the amount of contamination of mantle wedge derived magmas by crustal metasediments to about 10%. Reconstruction of initial magmatic stratigraphy has been carried out using CIPW-norms for cumulitic sequences within the massif, indicating a normal igneous polarity from west to east. Published geochemical signatures along the Pan-African suture zone of the Dahomeyides, in Ghana, Togo and Benin, constrain the origin of mafic granulitic and eclogitic complexes. A distinction is made between bodies with mainly MORB signatures originated from the subducted WAC plate passive margin and those with magmatic arc signatures originated from the over-riding plate mantle wedge. This suggests that the closure of the oceanic domain between the WAC and the SMC from 640 to 610 Ma was mainly accommodated by oceanic subduction beneath the active continental margin, before Pan-African collision.
© 2006 Elsevier B.V. All rights reserved.

Keywords: Granulite; Continental magmatic arc; Cumulates; Pan-African; West Africa

1. Introduction

In Precambrian fold belts, lower crustal rocks are generally exposed over a large surface area and their significance is a key point for understanding Earth dynamics at that time. Granulite facies metamorphic rocks are gen-

* Corresponding author at: Laboratoire de Transferts Lithosphériques, CNRS-UMR 6524, Magmas et Volcans, Université Jean Monnet, 23 rue Dr. P. Michelon, 42023 Saint Étienne Cedex 2, France. Fax: +33 4 77 48 51 08.
E-mail address: guillaume.duclaux@univ-st-etienne.fr (G. Duclaux).

0301-9268/$ – see front matter © 2006 Elsevier B.V. All rights reserved.
doi:10.1016/j.precamres.2006.08.012

erally considered to be deep seated continental crust and granulitic metamorphism as resulting from collision processes, crustal thickening and thermal relaxation (Harley, 1989). However, granulites may also form from underplated magmas equilibrated either in extensional regimes (attenuated continental lithosphere) or in active continental margin environments, at the deeper levels in the magmatic arc. Therefore, the understanding of the early stages of Precambrian orogens is greatly improved by the knowledge of the protolithic igneous features of granulites. Along the Pan-African Dahomeyides suture zone, between the West African Craton (WAC) and the Sahara Metacraton (SMC) several mafic granulitic massifs (Ménot, 1980; Bessoles and Trompette, 1980; Caby, 1989) are exposed. Among these, the Kabyé massif is one of the largest (~500 km^2) and its origin remains a matter of debate.

Arc magmatism occurs in convergent systems during ocean closure; calc-alkaline magmas are emplaced into the continental crust in an active continental margin or built as an intra-oceanic island in an intra-oceanic system. The chemistry of arc magmas is well understood with Large Ion Lithophile Elements (LILE) and High Field Strength Elements (HFSE) partitioning as Ti, Nb, Ta depletion controlled by ilmenite, rutile and sphene retained in the source (Wilson, 1989; Hawkesworth et al., 1993; Arculus, 1994). Nevertheless, distinctive chemical characteristics and related discrimination diagrams for determining tectonic setting are applicable only for rocks which represent liquid and not rocks with cumulitic features, i.e. rocks resulting from crystal accumulation and contain a more or less amount of residual liquids; such methods are not appropriate for cumulates which are about five times more volumetrically important, and constitute the most significant part of the arc root system (Wilson, 1989).

The present paper is mainly based on new geochemical data, and the aim is to determine the original tectonic setting of the Kabyé Complex and to reconstruct its primary magmatic features such as the origin of the initial layered sequence of cumulates and the related sequence of crystallization. Despite a strong metamorphic and tectonic imprint, the geochemical signature is still a reliable marker of the early history of the Kabyé igneous layered complex within the frame of the Pan-African Dahomeyides orogen. In this paper, the rock types and metamorphic assemblages are briefly described. Geochemical data and petrological implications are discussed in order to define the original tectonic setting of the Kabyé complex and its geodynamic significance during Neoproterozoic times.

2. Geological setting

The Dahomeyides orogen of Western Africa is a Pan-African collision belt between the passive continental margin of the WAC and the SMC (Bessoles and Trompette, 1980; Caby, 1987; Affaton et al., 1991; Abdelsalam et al., 2002) (Fig. 1). The Pan-African belt in Togo and Benin has been subdivided in three main units (Affaton, 1990): the western external units (Buem and Attacora), the eastern internal units (Benino-Nigerian Precambrian basement) and, in between, the so-called Dahomeyides suture zone. This suture zone is well exposed from SE Ghana to NW Benin. Numerous ultramafic and mafic bodies are scattered trough the suture zone. These bodies display contrasting lithological and metamorphic features (Ménot, 1980; Ménot and Seddoh, 1985; Attoh et al., 1997; Agbossoumondé et al., 2001, 2004). Granulites, eclogites and amphibolites are tectonically associated. This paper will focus on granulites from the Kabyé igneous complex.

The Kabyé massif (Fig. 2a) is one of the largest mafic bodies (50 km × 25 km) within the Dahomeyides suture zone (Fig. 1). Neodymium TDM model ages between 1267 and 1409 Ma were obtained with a crystallization age for the mafic protolith around 640 Ma (U/Pb zircon; Bernard-Griffiths et al., 1991). Peak of granulite metamorphism obtained by Pb/Pb zircon was around 612 Ma (Affaton et al., 2000). Large scale structures are roughly monoclinal, dipping toward the east at about 30° and striking along a north-south direction (Fig. 2b). On its western part, the Kabyé massif was thrusted over the 2.0 Ga Kara orthogneisses and is itself overthrusted by the Paleoproterozoic gneisses of the Binah and Tchamba formations (Affaton et al., 1984 and personal observations). Thus, the Kabyé massif forms a 12 km thick granulitic tectonic lens inserted into the Precambrian basement. Internal north-south shear zones split the massif in two main units. Shear criteria indicates thrusting toward the west under amphibolitic facies conditions, between 600 and 580 Ma (Attoh et al., 1997).

3. Sample location and description of rock types

3.1. Sample location

Important field investigations have been carried out during the past 3 years on the Kabyé massif. Among selected 98 samples, 43 have been analysed for whole rock geochemistry (Fig. 2 and Table 1). In addition, eight samples from Affaton et al. (2000) have been added to our geochemical dataset. Discrimination of the geodynamic environment has been carried out only on mafic

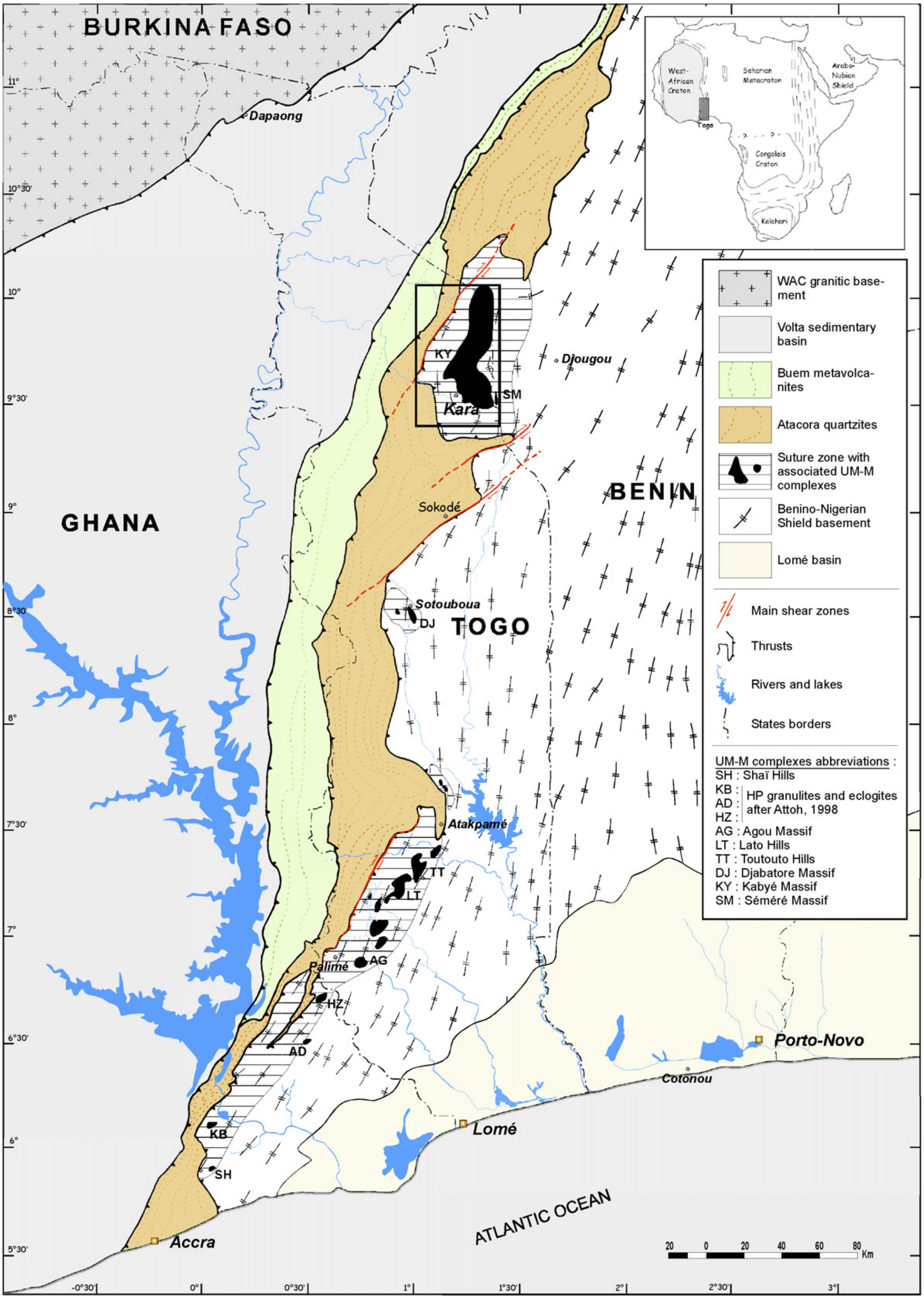

Fig. 1. Geological map of the Pan-African collision belt in Ghana, Togo and Bénin.

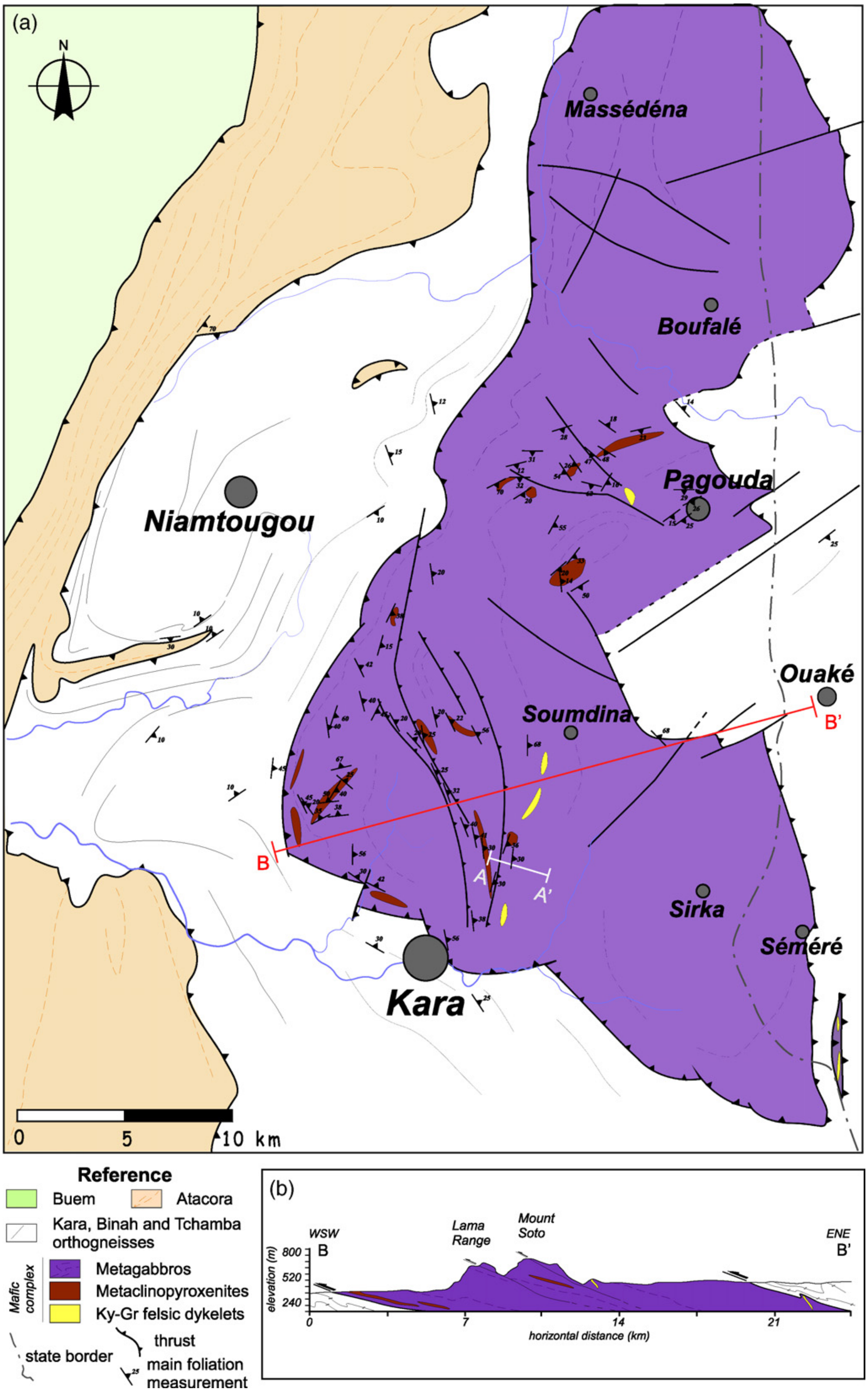

Fig. 2. (a) Geological and structural sketch map of the Kabyé massif showing the location of the A–A′ section used for the study of cumulates distribution (see text) and the B–B′ general section (b). (b) W–E cross section emphasizing the Pan-African nappe piling (vertical exaggeration 5×).

Table 1
Location of representative samples discussed in this study

Sample	Latitude longitude	Lithology
AF6436	09°38′570N 01°15′280E	Metagabbro
AF6451	09°44′300N 01°14′300E	Liquid
K17-1	09°38′125N 01°14′229E	Metapyroxenite
K17-4	09°38′805N 01°14′146E	Metagabbro
K17-12	09°37′611N 01°14′601 E	Metagabbro
K25-5	09°44′508N 01°16′322E	Liquid
TO64	09°39′157N 01°16′113E	Liquid
TO66	09°38′685N 01°15′307E	Metapyroxenite
TO69	09°37′812N 01°15′087E	Felsic dyke
TO70	09°36′600N 01°14′595E	Meta-anorthosite
TO72	09°35′652N 01°09′739E	Metagabbro
TO73A/D	09°35′773N 01°09′783E	Metapyroxenite
TO101B/C	09°35′638N 01°09′732E	Metagabbro
TO106	09°36′884N 01°08′850E	Metagabbro
TO107	09°36′634N 01°08′918E	Metapyroxenite
TO125	09°39′548N 01°12′600E	Metagabbro
TO132	09°36′167N 01°14′245E	Metapyroxenite
TO135	09°38′692N 01°15′378E	Metagabbro
TO136	09°38′120N 01°15′151E	Felsic dyke
TO138	09°39′050N 01°18′691E	Metagabbro
TO139	09°37′906N 01°19′044E	Metagabbro
TO140	09°35′918N 01°18′583E	Metagabbro
TO144B	09°46′340N 01°14′506E	Metapyroxenite
TO153	09°45′879N 01°19′486E	Metagabbro
TO174	09°43′625N 01°15′826E	Metapyroxenite

samples with non-cumulitic features (parts 4.1–4.3). Some samples have been selected to assess the origin and paleogeometry of the massif (part 4.6), they are distributed along a cross-section A–A′, in the southern part of the massif near Soumdina (from NW to SE: TO67, K17-4, K17-1, K17-12, TO132, AF6436, TO66 and TO70). This section has been selected because its cross cut the main foliation strike and displays good sample coverage, weak deformation and well preserved inherited modal layering features.

3.2. Rock types and layered series

Kabyé massif is mainly made of mantle-derived mafic rocks. Most of them are cumulates of metagabbros and metapyroxenites with preserved igneous textures in spite of granulite facies metamorphism. Moreover, the primary, magmatic, layering of cumulates may be still recognized in spite of later crosscutting granulitic foliations (Fig. 3a and e). Three main rocks types have been identified within the layered series: (i) ubiquitous layered meso to leucocratic metagabbros; (ii) dark garnet bearing and garnet free metaclinopyroxenites which are interlayered and intrusive within the metagabbro banded series and (iii) kyanite–garnet-bearing leucocratic dykelets.

3.2.1. Metagabbros series

They are characterized by Grt–Cpx–Pl ± Opx (minerals symbols after Kretz, 1983) (TO129, TO125 and TO72) or Opx–Cpx–Pl (TO138, TO139 and TO140) granulitic assemblages with subordinate rutile and quartz. The former assemblage is observed everywhere in the massif, while the second is restricted to the eastern part of the massif. Grt appears as coronas around both Ca-rich and -poor-pyroxenes. Duclaux et al. (2004) summarized their *P*–*T* evolution; the occurrence of relict Opx indicates initial metamorphic conditions of a maximum of 9 kbar, 900 °C after magmatic intrusion. Metamorphic peak conditions are estimated at 18 ± 3 kbar and 850 ± 20 °C in the SW unit and 12 ± 2 kbar at 775 ± 15 °C in the NE unit (Fig. 2). Localized retrogression under amphibolite facies conditions in both units is characterized by crystallization of pargasitic amphibole, secondary plagioclase, ilmenite and zoisite, at 9 ± 1 kbar and 775 ± 25 °C.

Most of the metagabbros display a striking layering which is marked both by a thin millimetric metamorphic banding with alternation of plagioclase and ferromagnesian-rich layers and by a thicker centimetre to decimetre compositional layering with the succession of dominant Cpx–Gt–Pl bearing facies and subordinate Opx–Cpx–Pl (Gt free) paragenesis. Such a feature probably reflects an inherited compositional magmatic layering which is superimposed by a secondary subconcordant regional metamorphic foliation (Fig. 3e). Deformation features are seen as Cpx and Gt porphyroclasts together with a mineral stretching lineation underlined by Cpx and garnet alignment (Fig. 3b, c and e).

3.2.2. Metapyroxenites

These melanocratic facies are coarse grained and generally present a weaker deformation imprint compared with metagabbros. Two types are distinguished with reference to the presence of garnet or not.

Grt-bearing metapyroxenites (TO107, TO64) outcrop in the western and northern parts of the massif (Fig. 2 and Table 1) and they occur as less foliated layers or elongated enclaves within the Grt-bearing metagabbros (see above) country rocks. Contacts are sharp and probably represent inherited magmatic contacts (Fig. 3a and b). They are coarse grained Cpx–Grt–Ilm bearing rock types and were previously described as eclogites or eclogitoïds (Affaton et al., 1984; Caby, 1987; Bernard-Griffiths et al., 1991; Castaing et al., 1993) but they rather correspond to HP granulites (Duclaux et al., 2004). Localized retrogression leads to clinopyroxene recrystallization and neoformed pargasitic amphibole, rare plagioclase and quartz.

Fig. 3. (a, b, d and f) Field relationships (a) preserved magmatic layering and cross cutting granulitic foliation. Dark and leucocratic layers, respectively, correspond to metapyroxenite and metagabbro; (b) Grt-bearing metapyroxenite as a boudinaged enclave within the Grt-bearing metagabbros; (d) Ky–Grt bearing felsic dykelet within the Grt-bearing metagabbros in the Séméré massif. Original igneous contacts are cross cut by the granulitic foliation visible on the right-hand side of the felsic dykelet; (f) mineralogy and texture of the granulitic Ky–Grt-bearing felsic gneiss; c and e: thin sections (c) partially retrogressed granulitic metagabbros with relict coronas (granulite facies: Grt 2 around Cpx) and totally transformed plagioclase (ampibolite facies: zoisite + secondary plagioclase + Grt); (e) granulitic foliation that transposed an earlier magmatic layering. Layering is underlined by alternating bands of contrasted modal composition that give, respectively, Cpx–Grt–Pl and Cpx–Opx–Pl assemblages in granulitic conditions.

Grt-free metapyroxenites (TO174, TO 144b) occurred only in the north-eastern part of the massif (Fig. 2 and Table 1). They contain a granulitic assemblage with large euhedral Opx surrounded by a granoblastic matrix of Cpx, Ilm and Cr–Spl. The retrogression is also characterized by pargasitic amphibole crystallization.

3.2.3. Kyanite–Garnet (Ky–Grt)-bearing felsic dykelets

Al-rich felsic rocks (TO69, TO 136) are very scarce and occurred in the central and eastern parts of the massif (Fig. 2 and Table 1) as decimetre patches and dykelets in the granulitic metagabbros. Relationships with the surrounding metagabbros are better exposed in the Séméré area (Benin, East of Kabyé) where the Ky–Grt-bearing rocks appears as dykelets of several cm in thickness (Fig. 3d) that cross cut the igneous layering of gabbros. Therefore they were certainly derived from Al-rich leucocratic felsic melts. They are coarse grained and contain a Qtz, Kfs, Grt, Ky granulitic assemblage (Fig. 3f). Kyanite crystallizes in the Qtz–Kfs matrix as well as inclusions within garnets. Retrogression is restricted to the crystallization of Bt.

4. Geochemical data and interpretations

4.1. Analytical methods

Major and minor elements concentrations were determined by XRF analyses at University of Lyon 1 (CNRS-UMR 5570); a set of 51 analyses has been used for this study. Analytical uncertainties (2σ) ranges from ±1% to ±2% for major elements; ±5% for trace elements when abundances ≥10 ppm, and ±10% for those ≤10 ppm. REE, Nd and Sr isotopes analyses were performed using the UMR CNRS "Magmas et Volcans" facilities (ICP-AES and TIMS) at University Jean Monnet and the School of Mines in Saint Etienne, and at University Blaise Pascal of Clermont Ferrand, respectively. Samples were dissolved using acid ($HF + HNO_3$, 1:3) in sealed Savillex beakers on a hot plate for 1 week. Method used was able to dissolved zircons and other refractory minerals to avoid trace elements fractionation. Separation of REE was done through a cation-exchange column (AG50WX8, 200–400 mesh). Sm and Nd were further purified using a second cation-exchange column, conditioned and eluted with dilute HCl. Isotopes analyses were performed using a VG 54E mass spectrometer. Replicate analyses of NBS987 yield a mean $^{87}Sr/^{86}Sr$ ratio of 0.710255 (S.D. = 12×10^{-6}, n = 9) and AMES a mean $^{144}Nd/^{143}Nd$ ratio of 0.511971 (S.D. = 6×10^{-6}, n = 8). Further analyses from Bernard-Griffiths et al. (1991) have been added to our set of isotopic data. Complementary data are reported from Affaton et al. (2000) with samples specified as AF (Table 1).

4.2. Identification of reliable indicators for geochemical interpretation

The entire magmatic suite underwent extensive recrystallization into granulite facies or locally in amphibolite facies conditions during the Pan-African orogeny. Nevertheless, no secondary mobilisation due to CO_2 and/or aqueous fluids seems to have significantly disturbed the initial magmatic element distribution. For example, LILE, such as K, Rb, Sr and Ba which are known to be easily removed, appear to have been relatively inert during the post-solidus evolution as they show neither erratic variations nor any significant covariations with alteration index (LOI). Furthermore, K/Rb ratio in felsic rocks ranges between 250 and 320 corresponding to typical continental crust values. REE spectra are consistent and homogeneous for each type of rocks (liquids, pyroxene cumulates and plagioclase cumulates) underlining the absence of late remobilisation for these elements. The generally strong negative correlation between highly incompatible elements such as LREE, Nb, Zr, Y, Ti and highly compatible elements such as MgO, Cr and Ni is also consistent with igneous processes. Na values are very low for felsic samples. This two samples come from two different parts of the massif and however present similar geochemical signatures arguing for a Na source depletion rather than mobility. Therefore, LILE may be used, together with HFSE as reliable indicators to define the magmatic processes responsible for the Kabyé complex genesis and to appraise its original tectonic setting.

4.3. Screening of cumulates and liquids

Field and microscopic observations suggest that most of the mafic rocks from the Kabyé massif are cumulates. Their crystallization is mainly related to crystal accumulation processes and to the more or less extensive extraction of residual liquids. Thus, screening of samples with liquid (non-cumulitic) or cumulitic characteristics is essential; liquids may be either initial, before cumulation, or residual, after cumulate formation. In that scope, are considered as "cumulates", rocks that deviate significantly from a true melt composition due to crystals accumulation (Pearce and Peate, 1995). Zr appears as a good index according to its highly incompatibility and therefore enrichment in residual liquids and depletion in cumulates (Rollinson, 1996). Thus, 22 samples with Zr contents higher than 50 ppm have been considered as potential liquids. These samples were plotted in a TiO_2 versus Al_2O_3 diagram (Pearce, 1996b) (Fig. 4). Three samples plotting in the field of liquids (AF6451, K25-5 and TO64) have been used to define magmatic affinity of

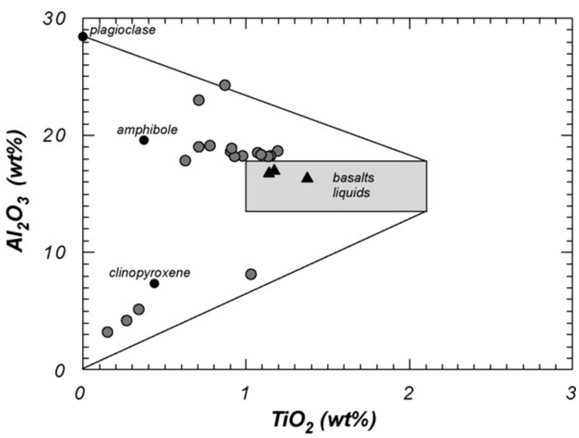

Fig. 4. Al_2O_3 vs. TiO_2 diagram (Pearce, 1996b) for screening between cumulates (grey dots) and liquid (black triangles) compositions of mafic rocks (SiO_2 ranging from 51 to 56%). Black dots: mean compositions of minerals of the Kabyé massif. Data from Table 2.

mafic magmas (major, trace elements) (in parts 4.1 and 4.4).

All the remaining samples have been considered as cumulates and some were used to constrain the initial geometry of the magmatic chamber. Both cumulates and liquids compositions as well as Al-rich felsic magmas (Gr–Ky bearing leucocratic dikelets) have been considered to assess magma mixing and crustal contamination in Sr/Nd isotopes diagram (part 4.5).

4.4. Geochemistry of magmatic liquids

4.4.1. Major and trace elements

Table 2 lists major and trace elements concentrations of samples representing mafic magmatic liquids and of the felsic samples (Ky–Gt bearing leucocratic dykelets). The three mafic samples form a homogenous set with SiO_2 ranging from 55.6 to 55.9 wt% corresponding to andesite compositions. They also display rather high Al_2O_3 (>16.4 wt%), intermediate CaO (6.8–7.4 wt%), Ni (<71 ppm) and Cr (<103 ppm) contents and intermediate Mg# (0.47–0.52), consistent with a relatively differentiated character for the magmatic suite. $FeO_{tot.}$ does not show any enrichment with differentiation and ranges from 7.6 to 9.0 wt%. According to Na_2O and K_2O contents, respectively, high (3.6–4.2 wt%) and moderate (0.5–1.5 wt%), and to intermediate to low (1.1–1.4 wt%) TiO_2 values suggesting early precipitation of Fe–Ti oxides, magmas may therefore be related to calc-alkaline series with high-alumina, medium-K affinities (Irvine and Baragar, 1971). In the $MgO–FeO_t–Al_2O_3$ diagram (Pearce et al., 1977) Kabyé analyses plot in the field of orogenic basalts, i.e. arc related magmas (Fig. 5a). Moreover in the Zr/Y–Zr diagram (Pearce, 1983) a continental arc origin is suggested (Fig. 5b).

The felsic samples display affinities with dacitic compositions and are characterized by high SiO_2 content and relatively low TiO_2 (63–67 wt% and 0.7–0.8 wt%, respectively), very low CaO and Na_2O (1.1–1.3 and 0.5–1.0 wt%) but high Al_2O_3 and K_2O (17.1–18.5 and 2.1–3.0 wt%) contents. Such K-rich felsic magmas strongly differ in origin from the closely associated mafic rocks. In fact, differentiation from a mafic magmatic source or partial melting of mafic rocks would have lead to Na-rich trondhjemitic liquids. For this reason and further isotopic data, Ky–Grt felsic dykelets may have been derived from a distinct source of continental origin (Rapp and Watson, 1995). Regarding their chemistry in the $Al/(Fe_t + Mg)$ versus $Ca/(Fe_t + Mg)$ diagram (Altherr et al., 1999) felsic magmas exhibit low Al and Ca ratios and plot in the field of metagreywackes. This suggests that the felsic melts derived from a continental protolith,

Table 2
Selected analyses of representative felsic and mafic rocks with liquid compositions

	Mafic liquids			Felsic magmas	
	AF6451	K25-5	TO64	TO136	TO69
SiO_2	55.88	55.58	55.93	63.33	66.64
TiO_2	1.14	1.17	1.37	0.79	0.74
Al_2O_3	16.89	17.11	16.42	18.46	17.07
Fe_2O_3	2.22	8.46	8.57	8.07	8.59
FeO	7.02	–	–	–	–
MnO	0.19	0.12	0.13	0.11	0.11
MgO	4.45	4.75	4.62	3.29	3.26
CaO	6.78	7.37	7.11	1.13	1.27
Na_2O	3.66	4.17	3.58	0.52	0.95
K_2O	1.22	1.24	1.45	2.97	2.08
P_2O_5	0.32	0.27	0.43	0.05	0.06
LOI	0.58	0.02	0	0.02	0
Total	100.13	100.26	99.59	98.78	100.84
Ba	442	375	580	688	564
Rb	17	26	30	98	55
Sr	407	520	511	62	72
Y	34	17	24	31	31
Zr	215	136	117	160	179
Nb	9	3	9	11	9
Th	–	–	2	2	4.5
Pb	–	7	9.2	0	1.5
Cu	111	206	164	33	19
Ni	30	59.7	71.3	61	47.8
V	177	196.8	186	77.2	79.1
Cr	61	70	103	99	112
Hf	–	–	1.2	3.1	2.9
Sc	24	18.4	17.2	12.3	14.4
Co	115	32.3	29.4	19.9	16.3
U	–	–	0.49	0.52	1.0
La	–	14.6	27.1	24.7	37.2
Ce	–	42.1	64.8	38.8	72.1
Nd	–	22.4	35.4	17.1	24.8
Sm	–	4.9	6.0	5.0	4.9
Eu	–	1.3	1.7	1.4	1.7
Gd	–	4.5	5.0	5.5	4.3
Tb	–	–	0.8	0.9	0.9
Dy	–	3.8	3.8	5.7	4.4
Ho	–	–	0.7	1.1	0.9
Er	–	1.9	1.9	3.4	3.0
Tm	–	–	0.2	0.5	0.5
Yb	–	1.6	1.6	3.5	2.4
Lu	–	–	0.2	0.5	0.4
Mg#	0.47	0.53	0.52	0.45	0.43
Zr/Y	6.3	8.2	4.9	5.1	5.8
Ce/Yb_N	–	11	18	2.6	6.8
Ce/Sm_N	–	3	3.8	2	3.8
Sm/Yb_N	–	3.6	4.8	1.3	1.8

Normalization to MORB (Hofmann, 1988) and to ORG (Pearce et al., 1984).

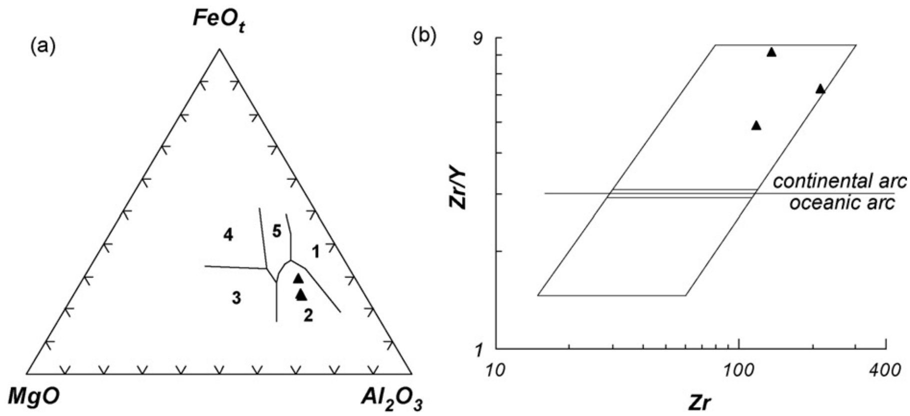

Fig. 5. Geochemistry of mafic rocks (SiO_2: 51–56%) and tectonic setting: (a) MgO–FeO_t–Al_2O_3 discriminant diagram (Pearce et al., 1977) ($n = 3$); 1: spreading centre, 2: island arc and active continental margin, 3: mid ocean ridge basalts, 4: ocean island, 5: continental basalts. (b) Zr/Y–Zr diagram (Pearce, 1983) distinction between continental and oceanic arcs magmas ($n = 3$).

and consequently have a different source than that of the mafic country rocks.

4.4.2. REE and incompatible element variations

N-MORB-normalized (Hofmann, 1988) incompatible element patterns for basic samples are presented in Fig. 6a. They display a nearly linear distribution characterized by decreasing abundances from LILE, Ba, Rb, Th and K down to HFSE. The regular slope is disturbed by a strong negative anomaly for Nb which is typical for magmas generated in the supra subduction mantle wedge. This fits well with relatively low Cr and Y contents (Pearce, 1982) and low Nb/Yb (2.3–6.8) ratios (Pearce and Peate, 1995). REE patterns are fractionated ($Ce/Yb_N \sim 11.0$–17.9) with slight LREE-enrichment ($Ce/Sm_N \sim 3.1$–3.8) and HREE depletion ($Sm/Yb_N \sim 3.6$–4.8) that could be induced by a garnet residue in the melt source. These features are typical for magmas directly derived from mantle in a subduction-related environment at depth greater than 90 km (Gill, 1981; Tatsumi et al., 1986; Tatsumi, 1989).

ORG-normalized (Pearce et al., 1984) incompatible element patterns for Al-rich felsic samples are presented in Fig. 6b. Relative to ORG, they present comparable values for Ce and Nb but are enriched in LILE and depleted in Zr, Hf and medium to heavy REE ($Ce/Sm_N \sim 2.0$–3.8 and $Ce/Yb_N \sim 2.6$–6.8). HREE are only slightly fractionated ($Sm/Yb_N \sim 1.3$–1.8). Such patterns display some similarities with arc related granites but the low Hf, Sm, Zr and Ce contents, together with high Rb values point out the continental crust derivation of the Al-rich felsic gneisses (Pearce et al., 1984; Pearce, 1996a). Moreover the moderately Th, K (and U, not plotted here) enrichment, compared to ORG, indicates

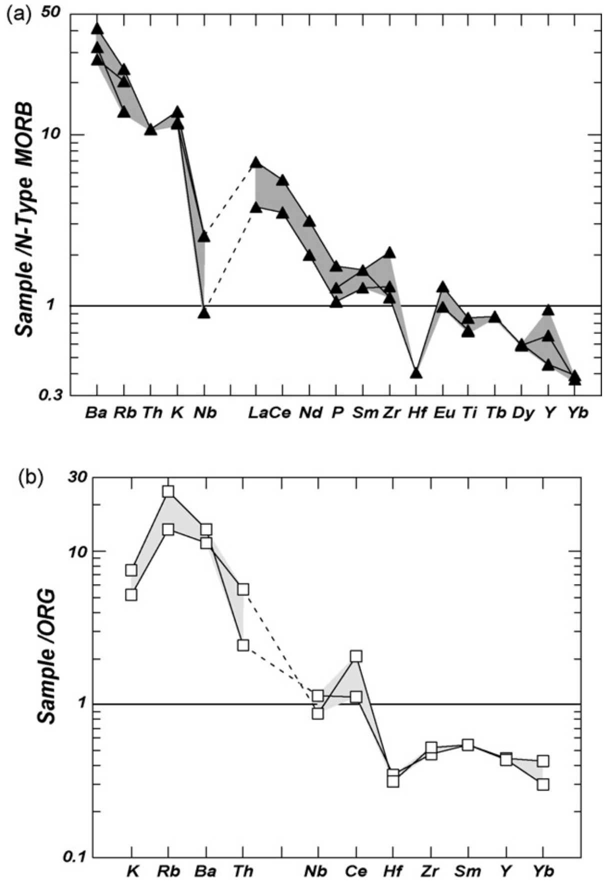

Fig. 6. Spiderdiagrams for mafic and felsic samples of the Kabyé massif: (a) mafic samples with liquid composition, normalization to N-MORB (Hofmann, 1988) ($n = 3$); (b) Ky–Grt bearing felsic dykelets, normalization to ORG (Pearce et al., 1984) ($n = 2$).

that source rock was probably not a material enriched in highly incompatible elements, such as the upper crust. The relative depletion in LREE and Nb also suggests a lower crustal source origin (Taylor and McLennan, 1985).

Even if felsic and mafic magmas display some similarity of composition such as LILE and LREE high contents, they also have striking geochemical differences. They are characterized, respectively, by concave REE patterns with no HREE fractionation and linear REE patterns with a regular decrease from LREE to HREE values (Table 2). Moreover, the mafic rocks, exhibit a striking Nb fractionation relative to other HFSE (Zr, Y, Hf: positive Zr/NbN). Furthermore, absence of a positive correlation between $\sum$REE and SiO_2 (as a differentiation index) for mafic and felsic samples argues for separate sources generating different magma compositions.

4.4.3. Sr and Nd isotopes

Measured ratios of $^{87}Sr/^{86}Sr$ and $^{143}Nd/^{144}Nd$ and epsilon values have been recalculated at 600 Ma and are presented in Table 3. Decay constants for Sm at $^{144}\lambda = 6.54 \times 10^{-11}$ and Rb at $^{87}\lambda = 1.42 \times 10^{-11}$ have been taking in account and present day CHUR values $^{143}Nd/^{144}Nd_{CHUR}{}^{0} = 0.512638$ and $^{147}Sm/^{144}Nd_{CHUR}{}^{0} = 0.1967$. Fig. 7 illustrates the first order dichotomy between mantle derived magmas corresponding to the mafic samples and crustal material corresponding to Ky–Grt felsic samples. Sample TO 153 represents the only mafic sample with negative ε_{Nd} value and is interpreted as a mix between the two poles. At a first approximation, this argues for at least two distinct sources.

All the mafic samples display positive ε_{Nd} values at 600 Ma, ranging between 0 and +9, except one which plots at −7. $^{87}Sr/^{86}Sr$ ratios are rather low and range from 0.7015 to 0.7051. Such a large dispersion of isotopic values for Sr and ε_{Nd} is indicative of the contamination of a LREE depleted mantle, reflecting either an enrichment of the mantle wedge by fluids derived from subducted metasediments and/or a later contamination by continental country rocks during the magma emplacement and crystallization (crustal contamination by the arc basement). Nevertheless the particular sample, TO153, with negative ε_{Nd} and close to zero ε_{Sr}, might be a good example of such a contaminated magma. The lack of correlation between the mafic ε_{Nd} and Nb values indicating that Nb negative anomaly described above is relative to the source composition rather than crustal contamination.

Felsic granulites point towards a clear crustal origin underlined by negative ε_{Nd} values, reflecting enriched source and very high ε_{Sr} values resulting from melting of crustal materials. The reference line proposed by DePaolo and Wasserburg (1979) separating materials derived from upper (high positive ε_{Sr}) to lower crust (low positive ε_{Sr}) has been plotted in Fig. 7. It suggests that felsic magmas may be derived from an old crustal component, possibly related to the surrounding Paleoproterozoic basement.

AFC calculations (DePaolo, 1981) have been carried out to model possible mixing between mantle and crustal sources (Fig. 7). Initial mantle source values for ε_{Nd} and ε_{Sr} have been chosen in agreement with the less differentiated mafic samples (high Ol normative), and with composition close to liquids to lower

Table 3
Nd and Sr isotope data for mafic (cumulates and liquids) and felsic rocks (in bold) of the Kabyé complex

Samples	Sm	Nd	Rb	Sr	$^{143/144}Nd$	$^{147}Sm/^{144}Nd$	$^{87/86}Sr$	$^{87}Rb/^{86}Sr$	$^{143/144}Nd_i$	ε_{Nd_i}	$^{87/86}Sr_i$	ε_{Sr_i}	T_{DM} (+10)
TO136	**4.97**	**17.12**	**98.1**	**62**	**0.511650**	**0.1755**	**0.780187**	**4.595500**	***0.51096***	***−17.7***	***0.74087***	***526.6***	**nd**
TO69	**4.89**	**24.79**	**54.7**	**72**	**0.511713**	**0.1192**	**0.762485**	**2.206778**	***0.51124***	***−12.1***	***0.74360***	***565.5***	**2.3 Ga**
TO153	3.78	15.69	4.3	482	0.512101	0.1456	0.703299	0.025789	*0.51153*	*−6.6*	*0.70308*	*−10.3*	2.3 Ga
TO 144b	0.3	1.1	1.3	10	0.512530	0.1649	0.704449	0.395792	*0.51188*	*0.3*	*0.70106*	*−38.9*	1.9 Ga
TO132	1.61	4.04	76.1	787	0.513006	0.2409	0.703887	0.279697	*0.51206*	*3.8*	*0.70149*	*−32.8*	nd
TO174	2.67	7.52	21.2	716	0.512926	0.2147	0.703519	0.085607	*0.51208*	*4.3*	*0.70279*	*−14.4*	nd
TO106	2.91	11.31	1.7	240	0.512669	0.1556	0.703936	0.020512	*0.51206*	*3.8*	*0.70376*	*−0.6*	1.26 Ga
TO135	4.16	17.17	1.7	458	0.512704	0.1465	0.703211	0.010741	*0.51213*	*5.2*	*0.70312*	*−9.7*	1.0 Ga
TO139	4.76	23.38	37.4	473	0.512549	0.1231	0.705573	0.228817	*0.51207*	*3.9*	*0.70362*	*−2.7*	1.0 Ga
TO101b	1.04	4.49	2.5	411	0.512557	0.1400	0.703484	0.017477	*0.51201*	*2.8*	*0.70333*	*−6.6*	1.23 Ga
TO64	6.04	35.41	30	511	0.512580	0.1031	0.704581	0.169706	*0.51217*	*6.1*	*0.70313*	*−9.6*	nd
TO66	6.55	22.86	1.3	32	0.512743	0.1732	0.706146	0.118632	*0.51206*	*3.9*	*0.70513*	*18.9*	1.53 Ga
TO67	1.05	2.76	1.2	26	0.513031	0.2300	0.703642	0.131459	*0.51213*	*5.1*	*0.70252*	*−18.3*	nd
TO73A	0.5	1.63	2.2	38	0.513074	0.1855	0.703445	0.165690	*0.51234*	*9.4*	*0.70203*	*−25.2*	nd
TO73D	0.7	2.81	1.9	62	0.512743	0.1506	0.703326	0.089057	*0.51215*	*5.6*	*0.70256*	*−17.6*	nd

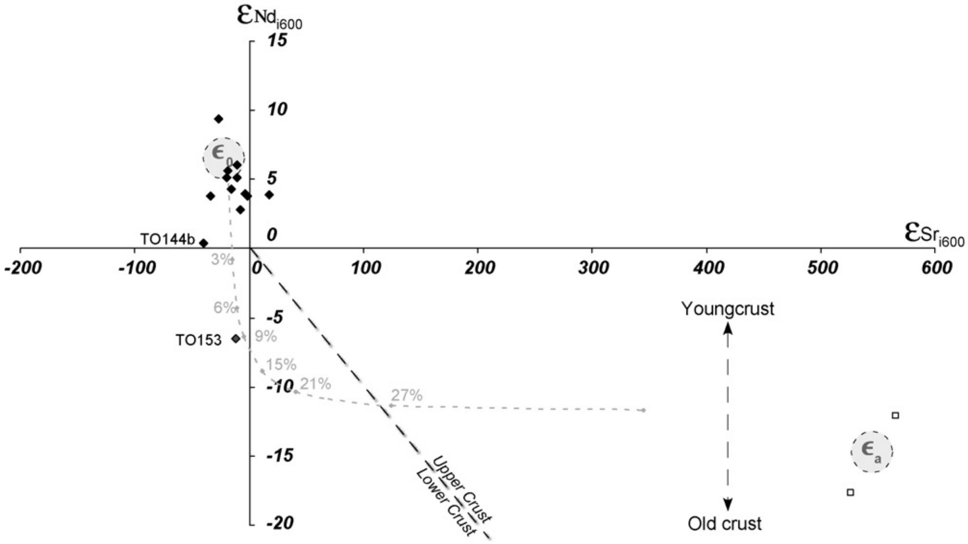

Fig. 7. ε_{Nd} vs. ε_{Sr} diagram and interpretation of relationships between the mafic–felsic rocks from the Kabyé massif; AFC mixing curve after DePaolo (1981). Black diamonds: mafic rocks (cumulates and liquids compositions); empty squares: Ky–Grt bearing felsic gneiss. The line separating materials derived from upper (high positive ε_{Sr}) to lower crust (low positive ε_{Sr}) have been proposed by DePaolo and Wasserburg (1979).

the influence of mineral segregation on the Rb, Sr, Sm and Nd elements contents. The crustal contaminant corresponds to mean values from the Ky-bearing granulitic gneisses. Tests have been done with slightly different ε values corresponding to a more primitive source, but calculations differ only by about 1–3% of contamination. Bulk partition coefficient D_{Nd} and D_{Sr} have been calculated taking in account proportions of normative plagioclase, clino- and orthopyroxene, and olivine from an average primitive liquid (values from Philpotts and Schnetzler, 1979). Modelling results suggest that magmas derived from the mantle wedge were contaminated by crustal material as suggested by sample TO153. Few samples reflect this mixture and the relatively low SiO_2 content of basic samples could not be explained by important crustal contamination. In those conditions, ~10% of crustal contamination is required to explain the most contaminated TO153 isotopic values.

T_{DM} model ages recalculate for actual Nd upper mantle at +10, give two groups of ages. The first group, obtained on the mafic rocks, ranges between 1.5 and 1.0 Ga as previously obtained by Bernard-Griffiths et al. (1991) and can be interpreted as depleted mantle source derivation age. The felsic melt (TO69) gives a T_{DM} at 2.3 Ga, suggesting that this rock derived from a Paleoproterozoic continental crust. Two mafic rocks (TO153 and TO144b) also give T_{DM} between 2.3 and 2.0 Ga, suggesting crustal contamination by an old continental component.

A continental arc system would be a convenient setting for crustal contamination of mafic magmas deriving from an enriched mantle source such as the suprasubduction mantle wedge. The base of the continental arc, built up by older gneisses could represent both a possible contaminant for ascending mafic magmas, and a source for the Al-rich felsic magmas.

4.5. Cumulate variation within the layered magmatic sequence

Within igneous layered complexes, the upwards succession of cumulates represents a reliable record of the mineralogical sequence of crystallization that occurs during cooling and solidification of a magmatic chamber. Therefore it reflects variations through time of the magma composition, of the crystallization parameters as P, T or fO_2 and also of the dynamic evolution of the magmatic chamber as open and/or closed system with periodic refilling by primitive magma and mixing between more and less differentiated magmas (Langmuir, 1989). In the Kabyé massif, mafic granulites show an obvious and spectacular cm to dm layering, especially at the outcrop scale, interpreted as an inherited magmatic feature (Fig. 3a).

If secondary metamorphic transformations did not significantly affect the original magmatic composition of protoliths (cf. above and Bernard-Griffiths et al., 1991), granulites chemistry, through CIPW norm calculations, should be used to assess primary mineralogy of cumu-

Table 4
Selected analyses of representative samples from the cumulitic sequence of the Kabyé complex

	TO67	K17-4	K17-1	K17-12	TO132	AF6436	TO66	TO70
SiO_2	49.46	53.12	51.35	60.67	48.57	55.38	44.65	49.34
TiO_2	0.47	1.19	0.34	0.93	0.68	1.10	1.55	0.45
Al_2O_3	6.67	18.74	5.16	17.31	8.06	18.44	13.73	27.62
FeO_t	10.96	7.96	8.69	5.61	10.59	7.29	15.69	3.10
MnO	0.20	0.14	0.18	0.11	0.19	0.12	0.20	0.04
MgO	18.75	4.67	20.00	2.80	15.84	3.87	10.33	1.47
CaO	12.17	8.48	14.00	5.24	15.16	8.10	11.70	13.63
Na_2O	0.44	4.23	0.23	4.35	0.64	4.24	0.93	3.15
K_2O	0.01	0.59	0.03	2.09	0.03	0.88	0.07	0.22
P_2O_5	0.01	0.31	0.01	0.24	0.01	0.15	0.02	0.08
LOI	0.00	0.00	0.00	0.35	0.00	0.46	0.00	0.16
Total	100.14	100.13	100.84	100.32	100.85	100.31	100.16	99.60
$X_{Fe} \times 100$	36.89	63.02	30.29	66.71	40.07	65.32	60.30	67.83
$Ca_2O/(Na_2O+K_2O) \times 100$	27.04	1.76	53.85	0.81	22.63	1.58	11.70	4.04
Mg#	0.58	0.33	0.65	0.29	0.55	0.30	0.35	0.28
Al_2O_3/MgO	0.36	4.01	0.26	6.18	0.51	4.76	1.33	18.79
CIPW norm								
Q	2.22	4.04	2.10	13.26	0.64	4.67	3.82	0.44
Or	0.06	3.48	0.18	12.37	0.18	5.21	0.41	1.31
Ab	3.71	35.64	1.93	36.78	5.36	35.89	7.81	26.77
An	16.12	30.27	12.82	21.50	18.83	28.69	32.84	60.84
Ab + An	19.83	65.91	14.75	58.28	24.19	64.58	40.65	87.61
Di	34.20	7.68	43.48	2.42	43.25	8.66	19.24	5.23
Hy	30.87	8.08	29.39	5.88	19.21	10.45	16.76	1.28
Ol	0.00	0.00	0.00	0.00	0.00	0.00	0.00	0.00
Mt	0.65	0.46	0.58	0.36	0.62	4.01	0.65	0.13
Hm	11.69	8.51	9.17	5.98	11.24	0.00	16.88	3.37
Il	0.00	0.00	0.00	0.00	0.00	2.09	0.00	0.00
Ap	0.02	0.67	0.02	0.52	0.02	0.33	0.04	0.18

lates. Taking into account the spatial location of samples, a first attempt has been made in order to constrain the distribution of cumulates within the complex, and if possible to recognize an inherited igneous stratigraphy and igneous crystallization order.

Table 4 lists the major and trace elements concentrations of some representative samples of cumulates. Related CIPW-norms were calculated using the method of Irvine and Baragar (1971).

As shown by Bernard-Griffiths et al. (1991), REE patterns of Kabyé cumulate rocks reflect the proportions of the major cumulus minerals. Two different types of REE patterns are distinguished (Fig. 8), which are related to dominant crystallization of Pl (anorthositic type) and Cpx (clinopyroxenitic type). This clearly underline the difficulty of using cumulates to assess magmatic sources and tectonic settings of mafic layered complexes. In fact, their geochemical signatures (except isotopes) reflect mainly physical mechanisms controlling both crystals settling and segregation (concentration) and melt extrac-

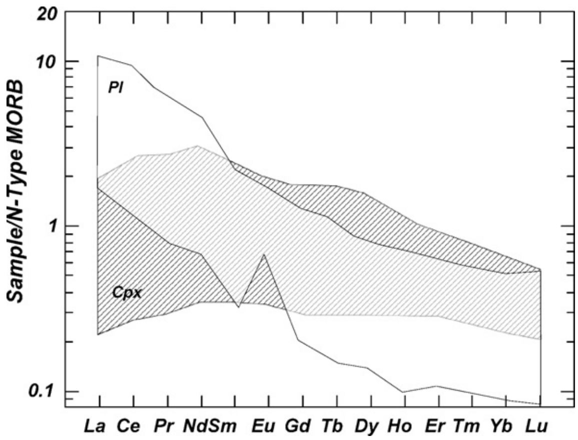

Fig. 8. REE patterns of cumulates of the Kabyé massif emphasizing that whole rock composition is closely controlled by the dominant crystallization of plagioclase and clinopyroxene. For example the La/Nd ratio are, respectively, highly positive for Pl-rich cumulates and negative for the Cpx-rich cumulates. Furthermore, a positive Eu anomaly characterized the Pl-rich cumulates. Normalization to N-MORB (Hofmann, 1988).

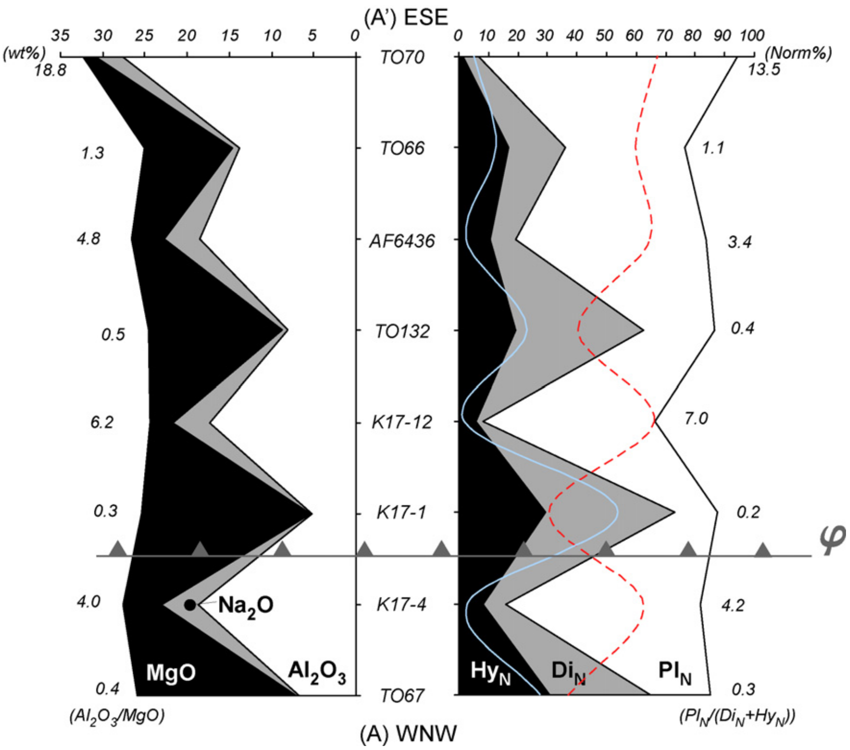

Fig. 9. Chemical cryptic and normative variation of cumulates composition along section A–A′ (Fig. 2a) showing the cyclic crystallization of ferromagnesian and feldspar minerals as well as a general differentiation trend towards the East, i.e. the top of the section. Italic numbers correspond to the Al_2O_3/MgO ratio (left) and to $Pl_N/(Di_N + Hy_N)$ ratio (right). Dashed and continuous lines represent variation of, respectively, $X_{Fe} \times 100$ and $CaO/(Na_2O + K_2O) \times 100$. φ possible thrust disturbing the original igneous layering of cumulates.

tion rather than chemical processes dominated by partial melting and fractional crystallization, i.e. processes related to geodynamic environment.

4.5.1. Major elements and modal variations of cumulates at a local, kilometric scale

Variation diagrams (Fig. 9) have been used to constrain evolution of a sequence of cumulates along the A–A′ section in the southern central part of the massif (Fig. 2). This section of about 2 km long cuts across the main layering strike. Samples are separated of hundreds of metres and indicate sequential crystallization of cumulates with a global differentiation polarity from NW to SE. This section (Fig. 2) does not represent an exhaustive sampling of each layer but may be considered to reflect medium scale variations into the complex. From NW to SE, CIPW variations indicate a sub-regular alternation of mafic melanocratic bands (TO67, K17-1, TO132 and TO66) and mafic to intermediate leucocratic bands (K17-4, K17-12, AF6436 and TO70), respectively, dominated by pyroxene and plagioclase as the dominant cumulitic phase. In the same way, the section displays a global evolution marked by increasing normative plagioclase (Pl_N), coupled with decreasing normative Orthopyroxene (Hy_N) and Clinopyroxene (Di_N) contents. This could be interpreted as a bottom (NW) to top (SE) trend of differentiation. But an anomaly is noted by the more primitive composition of sample K17-1 relative to TO67. Either a re-injection event or a tectonic repetition could have been responsible for this local inverted igneous polarity. According to field observations and structural mapping, the tectonic duplication seems to be the best explanation. The base of the cumulates section is close to a major thrust (Fig. 2) and several hundreds metre scale folding, or thrusting, is likely to have occurred and disturb the initial magmatic sequence. Therefore, if TO67 is replaced by K17-1 at the base of the sequence, an inverse correlation of normative proportions, decreasing Hy_N and Di_N and increasing Pl_N can be observed.

Moreover, at the scale of the A–A′ section, chemical cryptic variations may be reported: the Al_2O_3/MgO ration increase from bottom to top, indicating sequential fractional crystallization of ferromagnesian and feldspar phases. In the same way, X_{Fe} increases, marking Mg depletion into ferromagnesian phases that is characteristic of magmatic series evolution. $CaO/(K_2O + Na_2O)$

ratio also decreases, controlled by crystallization of more and more sodic feldspars, another sign of magma differentiation.

In conclusion, cumulates seem to be more and more differentiated from West to East, pointing out a normal igneous polarity for the magmatic sequence. This magmatic feature may be locally disturbed by secondary tectonic structures such as thrusting with some duplication.

4.5.2. Major elements and modal variations at the scale of the Kabyé massif

Constraining large scale magmatic geometry for the A–A′ section has to be carefully undertaken due to late intra-body deformation under amphibolite facies metamorphic conditions. The Kabyé massif has been split into three different regions relative to large scale monoclinal structures. Samples from the western, central and eastern part of the massif are distinguished in Fig. 10.

A set of 44 chemical analyses of cumulates have been plotted in Fig. 10. A significant discrimination of the various cumulates may be carried out as they are scattered between the representative points of the four main minerals (plagioclase, clinopyroxene, orthopyroxene and olivine) that occur in various proportions. Most of the samples plot along the (FeO + MgO)–(Al_2O_3 + CaO) line, i.e. the olivine–orthopyroxene–clinopyroxene–plagioclase line, according to the mafic nature of parent magmas. Different types of cumulates are clearly discriminated: pyroxenites and olivine pyroxenites, gabbros and noritic gabbros, and anorthosites. If the location of samples within the massif is considered (Fig. 10a), it appears that (i) the lowermost (western) part is built up by mainly melanocratic cumulates, rich in Opx or Ol bearing gabbros and subordinate leucocratic gabbros, (ii) the middle part by less melanocratic cumulates, dominant gabbros and some anorthosites and (iii) the upper (eastern) part presents an homogenous petrological composition with dominant gabbros. Such a sample distribution demonstrates the eastwards differentiation trend of the Kabyé layered complex. This igneous polarity is also confirmed by the evolution of mineral chemistry as shown by the higher Na_2O contents of plagioclases (Fig. 10a) and higher FeO_t/MgO of pyroxenes (Fig. 10b) from cumulates from the middle and upper parts and from the lower part, respectively.

In the same way, the mineral crystallization sequence may be defined as Ol–Opx–Cpx–Pl as successive cumulus phases from parent magma. Such a sequence characterized by the late crystallization of feldspar is typical of calc-alkaline suites (Groves and Baker, 1984) and the early occurrence of Opx suggests a high silica activity

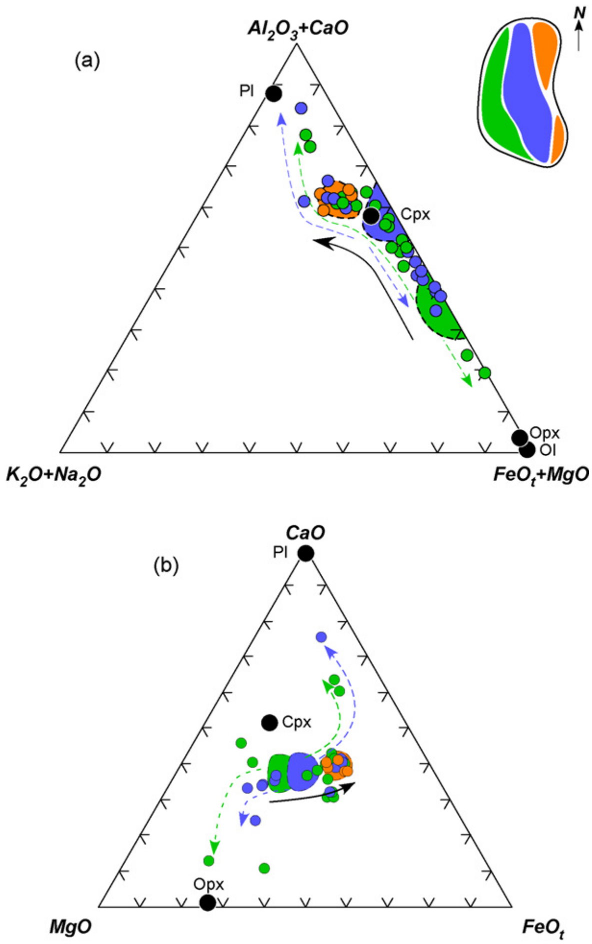

Fig. 10. Chemical evolution of the Kabyé complex cumulates. (a) ($K_2O + Na_2O$)/(Al_2O_3 + CaO)/(FeO_t + MgO) diagram showing the chemical evolution of cumulates of the Kabyé massif. Mean compositions of minerals have also been reported. Inset: sketch explaining the color code used for samples with respect to their location within the massif; green: western area (i.e. lowermost section of the complex), blue: centre and orange: eastern area (i.e. uppermost section). Dashed arrows correspond to differentiation trends into the different sections of the layered complex and the black arrow underlines the global differentatiton trend at the scale of the massif. Within each section, i.e. main sequences, the gap between pyroxenitic and plagioclasic cumulates probably reflects the composition of initial magmas (coloured field) before cumulates crystallization. At the scale of the complex, initial magmas look more and more evolved toward the East, i.e. the geometric top, indicating a global differentiation trend. (b) MgO/CaO/FeO_t diagram illustrating the eastward differentiation trend of cumulates as suggested by increasing FeO/MgO values of pyroxenes. Color code similar to (a).

(Beccaluva et al., 1984) may be in relation with crustal contamination.

Thus, the Kabyé layered complex can be considered as in situ crystallization of a single major magma chamber, with a differentiation polarity from west to east, i.e.

from bottom to top of the complex, and possibly derived from a unique parental magma.

5. Discussion

5.1. Origin of the Kabyé massif

5.1.1. Arc magmatism

The mafic rocks and their compositions emphasize the homogeneity of the entire massif in terms of its mantle origin. Major, trace and REE elements data indicate that the Kabyé mafic rocks have a magmatic arc signature. Furthermore, the lack of correlation between Nb and ε_{Nd} underlined that Nb depletion reflect a source characteristic confirming an arc environment for mafic rocks genesis. Considering the pressure of equilibration of parageneses (∼9 kbar), the Kabyé massif is a well preserved example of a typical mature arc with crustal thickness between 30 and 40 km (Green, 1992), i.e. the root of the magmatic arc.

5.1.2. Crustal contamination and continental arc origin

Occurrence of mainly cumulative mafic arc-related magmas indicates deep conditions of crystallization in accordance with thermobarometric estimations (Hilairet, 2004; Duclaux et al., 2004). Furthermore, Nd and Sr isotopes point out contamination processes of the arc-related magma chamber by up to 10% melts sourced from the continental crust. Source derivation age (T_{DM}) around 2.3 Ga for felsic melts suggest that these rocks derived from the Sahara Meta-Craton. Moreover, the mafic contaminated rocks with ε_{Nd} comprises between 0 and −7 have similar T_{DM} ages, underlining an interaction between mantle-derived component (positive ε_{Nd} younger T_{DM} 1.5–1.0 Ga) and the Sahara Meta-Craton.

Felsic melts, derived from melting of primary continental crust would be produced by the intrusion of the mafic magma. Other example of such melting was proposed by McMillan et al. (2003) for the Neoproterozoic Ranomandry Complex in central Madagascar. This gabbro complex is also a calc-alkaline body with very subordinate felsic magma. The latter are restricted to the complex margins, and their mineralogy is compatible with that of the Kabyé felsic dykes in spite of a lower pressure equilibration, as indicated by the absence of Ky. As discussed by McMillan (op. cit.), the occurrence of a well preserved mafic body associated with granite magmas argues for a structurally homogeneous lower crust without important shear zones which would have drained away low density felsic magmas. Intrusion into the continental crust of a large high temperature magmatic mafic body could be a valuable heat source to trigger melting of the lower continental crust and then produce important migmatite terranes (Laube and Springer, 1998; Dufek and Bergantz, 2005).

5.2. Preservation of magmatic layering in a granulitic continental arc

The chemical composition and layering in the Kabyé magmatic arc have been described and indicate a typical calc-alkaline crystallization sequence with typical magmatic compositional features of in situ crystallization in the magma chamber. Moreover, the overall evolution within the massif from West to East, i.e. from bottom to top, reflects an original magmatic differentiation trend. Normal igneous polarity of cumulates indicates that the Kabyé complex has not been overturned but just tilted during Pan-African collision. Detailed study of the chemistry of the metacumulates seems to be a powerful tool for investigating metamorphic (but not altered) mafic rocks. Other examples of well-preserved high-grade magmatic arc rocks are known from the Jijal complex in Kohistan (Bard, 1983; Burg et al., 1998; Yamamoto and Nakamura, 2000) and Fiordland arc in New Zealand (Clarke et al., 2000). Comparable fragments of Pan-African magmatic arcs outcrop along the Braziliano Pan-African Belt further to the south (Campanha and Sadowski, 1999) and northward in Hoggar (Caby, 2003). Most of the examples have been studied specifically for their metamorphic assemblages and reactions. But, few relevant data are available regarding their geochemistry and the possible recognition and description of inherited magmatic features.

5.3. Comparison with other mafic and ultramafic massifs along the suture zone

Ultramafic and mafic massifs from the Dahomeyides suture zone, witness oceanic closure and amalgamation of Gondwana super-continent during Pan-African time between 640 and 540 Ma. Association of granulitic and eclogitic mafic bodies along a single suture zone reflects a tectonic mélange of different high grade rocks coming from both plates acting during subduction. Geochemical affinities and metamorphic evolution allow the distinction to be made between materials from the upper and lower plates in a subduction environment. As pointed out by Agbossoumondé et al. (2001), the Lato and Toutouto hills mafic complexes display MORB like geochemical signatures and a clockwise metamorphic evolution from eclogitic to granulitic and the retrogression to amphibolitic facies conditions between 610 and

580 Ma. Agbossoumondé (op. cit.) interpreted these bodies as exhumed fragments of the WAC margin previously subducted and metamorphosed under eclogitic facies conditions. Moreover, Agbossoumondé et al. (op. cit.) show that igneous protoliths of the Agou granulitic complex have REE characteristics of plagioclase cumulates, further supported by major element signature as well as trace elements contents, and displaying calc-alkaline affinities. Such geochemical features are consistent with an active continental margin environment, and very similar to the Kabyé complex environment. It is reasonable to consider the origin of the Agou massif is a magmatic body emplaced and cooled at the base of a continental crust in a supra subduction zone, as proposed in this paper for the Kabyé complex. Considering the dominantly westward verging of the structures along the Dahomeyides suture zone (Affaton, 1990; Attoh et al., 1997; Attoh, 1998; Agbossoumondé et al., 2004; this study) and the occurrence of eclogitic bodies with WAC affinity, it has been proposed that the initial subduction plane was dipping eastward, beneath the Benino-Nigerian shield. Thus, in this global tectonic context, the Kabyé and the Agou massifs developed on the western continental active margin of the SMC.

Further to the South, Attoh and Morgan (2004) compare granulitic and eclogitic mafic bodies along the Dahomeyides suture zone in Togo and Ghana. But the authors do not clearly separate the magmatic complexes deriving from the over-riding and the subducted plates, respectively. However, from a geochemical point of view, most of the analyses cannot be used in the appropriate discrimination diagrams because a number of them correspond to cumulate rather than to liquid compositions. Only two samples with liquid composition (KB65 and KB67) can be clearly identified according to our criteria. Considering the lack of Ta depletion, an arc source for these magmas is debatable. Furthermore, without isotope data, island arc affinities of the magma cannot be attested fully. Thus, for a better understanding of the Pan-African orogeny, it will be essential to acquire an improved geochemical knowledge of the high grade mafic rocks from SE Ghana but also northwards from Derouvarou, North Benin (Aicard, 1957) and Amalaoulaou in the Gourma region of Mali (La Boisse, 1979) where, today no detailed geochemical studies have been completed.

6. Conclusion

This petrological and geochemical study of the Kabyé massif places important constraints on the origin of granulitic rocks along the Dahomeyides suture zone, and more generally concerning the origin of large-scale Pan-African metamorphic terranes worldwide. We demonstrate that the Kabyé massif corresponds to the root of a continental arc mainly built up by plagioclase or clinopyroxene bearing metacumulates with very subordinate crosscutting felsic melts of continental origin. Modelling of isotopic data suggests that some mafic rocks may result from contamination of mantle wedge derived magmas by crustal materials from the Saharan Meta Craton, i.e. assimilation of felsic material, up to a maximum of 10%. In spite of a slight disturbance by later westward thrust tectonics, the original geometry of the magma chamber and the magmatic sequence of differentiation are well preserved. The layered complex displays more and more differentiated cumulates from west to east. A brief review of the available geochronological data suggests that the Kabyé massif developed between 640 and 610 Ma on the western margin of the SMC during eastward dipping subduction of the oceanic domain bordering the eastern passive margin of the WAC. Agou massif in South Togo is an other good example Further investigations, in Ghana, Benin and Mali, along this well preserved Pan-African subduction zone, and in Brazil, will improve in defining the timing and subsequent amalgamation of West Gondwana.

Acknowledgements

This research was financially supported by the Agence Universitaire de la Francophonie, and by CNRS UMR 6524 and UMR 5570. We warmly thank Prof. Peter Bowden and Christopher Harris (Cape Town) for discussion and corrections that greatly improve the present manuscript. Many thanks also to the two anonymous reviewers for their constructive reviews.

References

Abdelsalam, M.G., Liégeois, J.-P., Stern, R.J., 2002. The Saharan Metacraton. J. Afr. Earth Sci. 34, 119–136.

Affaton, P., 1990. Le bassin des Volta (Afrique de l'Ouest): une marge passive du Paléoprotérozoïque supérieur, tectonisée au Panafricain (600 ± 50 Ma). Thèse d'Etat, vol. 2, 499 p., ORSTOM Ed., France.

Affaton, P., Laserre, J.L., Lawson, T.L., Vincent, P.L., 1984. Notice explicative de la carte géologique à 1/200,000 de Kara (République du Togo). Mémoire 1, Direction Générale des Mines et de la Géologie et Bureau National de Recherches Minières du Togo, 36 p.

Affaton, P., Rahaman, M.A., Trompette, R., Sougy, J., 1991. The Dahomeyide Orogen: tectonothermal evolution and relationships with the Volta basin. In: Dallmeyer, R.D., Lecorché, J.P. (Eds.), The West African Orogens and Circum-Atlantic Correlatives. Springer, New York, pp. 95–111.

Affaton, P., Kröner, A., Seddoh, K.F., 2000. Pan-African granulite formation in the Kabye Massif of northern Togo, West Africa: Pb–Pb zircon ages. Int. J. Earth Sci. 88, 778–790.

Agbossoumondé, Y., Ménot, R.P., Guillot, S., 2001. Metamorphic evolution of Neoproterozoic eclogites from south Togo West Africa. J. Afr. Earth Sci. 332, 227–244.

Agbossoumondé, Y., Guillot, S., Ménot, R.P., 2004. Pan-African subduction-collision event evidenced by high-P coronas in metanorites from the Agou massif (southern Togo). Precambrian Res. 135, 1–21.

Aicard, P. 1957. Le Précambrien du Togo et du Nord-Ouest du Dahomey. Doctoral Thesis. Univ. Nancy and Bulletin Direction fédérale Mines et Géologie, Dakar, 23, 226 p.

Altherr, R., Henjes-Kunst, F., Langer, C., Otto, J., 1999. Interaction between crustal-derived felsic and mantle-derived mafic magmas in the Oberkirch Pluton European Variscides, Schwarzwald, Germany. Contrib. Mineral. Petrol. 137, 304–322.

Arculus, R.J., 1994. Aspects of magma genesis in arcs. Lithos 33, 189–208.

Attoh, K., 1998. High pressure granulite facies metamorphism in the Pan-african Dahomeyide orogen, West Africa. J. Geol. 106, 236–246.

Attoh, K., Dallmeyer, R.D., Affaton, P., 1997. Chronology of nappe assembly in the Pan-African Dahomeyide orogen, West Africa: evidence from 40Ar/39Ar mineral ages. Precambrian Res. 82, 153–171.

Attoh, K., Morgan, J., 2004. Geochemistry of high-P granulites from the Pan-African Dahomeyide orogen, West Africa: constraints of the origin and composition of the lower crust. J. Afr. Earth Sci. 39 (3/5), 201–208.

Bard, J.P., 1983. Metamorphism of an obducted island arc; example of the Kohistan sequence Pakistan in the Himalayan collided range. Earth Planet. Sci. Lett. 65, 133–144.

Beccaluva, L., Ohnenstetter, D., Ohnenstetter, M., Paupy, A., 1984. Two magmatic series with island arc affinities within the Vourinos ophiolite. Contrib. Mineral. Petrol. 85, 253–261.

Bernard-Griffiths, J., Peucat, J.J., Ménot, R.P., 1991. Isotopic Rb–Sr, U–Pb and Sm–Nd and trace element geochemistry of eclogites from the Pan-African Belt: a case study of REE fractionation during high-grade metamorphism. Lithos 27, 43–57.

Bessoles, B., Trompette, R., 1980. Géologie de l'Afrique. La chaîne panafricaine zone mobile d'Afrique centrale (partie sud) et zone soudanaise. Orléans, France, B.R.G.M. mém. 6.

Burg, J.P., Bodinier, J.L., Chaudhry, M.N., Hussain, S., Dawood, H., 1998. Infra-arc mantle-crust transition and intra-arc mantle diapirs in the Kohistan Complex (Pakistani Himalaya): petro-structural evidence. Terra Nova 10 (2), 74–80.

Caby, R., 1987. The Pan-African belt of West Africa from the Sahara to the Gulf of Benin. In: Schaer, J.P., Rogers, J. (Eds.), The Anatomy of Mountain Ranges. Princeton Series in Geology and Paleontology.

Caby, R., 1989. Precambrian terranes of Benin-Nigeria and northeast Brazil and the Late Proterozoic south Atlantic fit. Geological Society of America, Spec. Paper 230, pp. 145–158.

Caby, R., 2003. Terrane assembly and geodynamic evolution of central-western Hoggar: a synthesis. J. Afr. Earth Sci. 37 (3–4), 139–159.

Campanha, G.A. da C., Sadowski, G.R., 1999. Tectonics of the southern portion of the Riberia Belt (Apiai Domain). Precambrian Res. 98 (1–2), 31–51.

Castaing, C., Triboulet, C., Feybesse, J.L., Chevremont, P., 1993. Tectonometamorphic evolution of Ghana, Togo, and Benin in the light of the Pan-African/Brasiliano orogeny. Tectonophysics 218, 323–342.

Clarke, G., Klepeis, K., Daczko, N., 2000. Cretaceous high-P granulites at Milford Sound, New Zealand: metamorphic history and emplacement in a convergent margin setting. J. Metamorph. Geol. 18, 359–374.

DePaolo, D.J., Wasserburg, G.J., 1979. Petrogenetic mixing models and Nd–Sr isotopic patterns. Geochim. Cosmochim. Acta 43, 615–627.

DePaolo, D.J., 1981. Trace element and isotopic effects of combined wallrock Assimilation and Fractional Crystallization. Earth Planet. Sci. Lett. 53, 189–202.

Duclaux, G., Guillot, S., Agbossoumonde, Y., Ménot, R.P., Hilairet, N., Fernandez, A., 2004. The Kabyé granulitic massif (Northern Togo), a witness of a subducted and collided Pan-African arc. In: Proceedings of the 20th Colloquium of African Geology, Orléans, France, p. 146 (Abstracts volume).

Dufek, J., Bergantz, G.W., 2005. Lower crustal magma genesis and preservation: a stochastic framework for the evaluation of basalt–crust interaction. J. Petrol. 46, 2167–2195.

Gill, J., 1981. Orogenic Andesites and Plate Tectonics. Springer, New York.

Green, T.H., 1992. Anatexis of mafic crust and high presssure crystallisation of andesite. In: Thorpe, R.S. (Ed.), Andesites. John Wiley & Sons, Chichester, pp. 465–487.

Groves, T.L., Baker, M.B., 1984. Phase equilibrium controls on the tholeiitic versus calc alkaline differentiation trends. J. Geophys. Res. 89, 3253–3274.

Harley, S.L., 1989. The origin of granulites: a metamorphic perspective. Geol. Mag. 126, 215–247.

Hawkesworth, C.J., Gallagher, K., Hergt, J.M., McDermott, F., 1993. Mantle and slab contribution in arc magmas. Annu. Rev. Earth Planet. Sci. 21, 175–204.

Hilairet, N., 2004. Le massif granulitique HP de Kabyé (Nord Togo), témoin d'un arc continental impliqué dans l'orogenèse panafricaine. Unpublished DEA, University of Clermont Ferrand.

Hofmann, A.W., 1988. Chemical differentiation of the Earth: the relationship between mantle, continental crust, and oceanic crust. Earth Planet. Sci. Lett. 90, 297–314.

Irvine, T.N., Baragar, W.R.A., 1971. A guide to chemical classification of the common volcanic rocks. Can. J. Earth Sci. 8, 523–548.

Kretz, R., 1983. Symbols for rock-forming minerals. Am. Mineral. 68, 277–279.

La Boisse, H. de, 1979. Pétrologie et géochronologie des roches cristallophylliennes du bassin du Gourma (Mali): conséquences géodynamiques. Unpublished Thesis. University Montpellier, 54 pp.

Langmuir, C., 1989. Geochemical consequences of in situ crystallization. Nature 340, 199–205.

Laube, N., Springer, J., 1998. Crustal melting by ponding of mafic magmas. J. Volcanol. Geoth. Res. 81 (1–2), 3–19.

McMillan, A., Harris, N.B., Holness, M., Ashwal, L., Kelly, S., Rambeloson, R., 2003. A granite–gabbro complex from Madagascar: constraints on melting of the lower crust. Contrib. Mineral. Petrol. 145, 585–599.

Ménot, R.-P., 1980. Les massifs basiques et ultrabasiques de la zone mobile Pan-Africaine au Ghana, Togo et Bénin. Etat de la question. Bulletin de la Société Géologique de France 22, 297–303.

Ménot, R.P., Seddoh, K.F., 1985. The eclogites of the Lato hills, South Togo West Africa: relics from the early tectonometamorphic evolution of the Pan-African orogeny. Chem. Geol. 50, 313–330.

Pearce, J.A., 1982. Trace elements characteristics of lavas from destructive plate boundaries. In: Thorpe, R.S. (Ed.), Andesites: Orogenic Andesites and Related Rocks. John Wiley, pp. 525–548.

Pearce, J.A., 1983. Role of the sub-continental lithosphere in magma genesis at active continental margins. In: Hawkesworth, C.J., Norry, M.J. (Eds.), Continental Basalts and Mantle Xenoliths, pp. 230–249.

Pearce, J.A., 1996a. Sources and setting of granitics rocks. Episodes 19, 120–125.

Pearce, J.A., 1996b. A user's guide to basalt discrimination diagrams. In Wyman, D.A. (Ed.), Trace Element Geochemistry of Volcanic Rocks: Applications for Massive Sulphide Exploration. Geological Association of Canada, Short Course Notes 12, 79–113.

Pearce, J.A., Harris, N.B.W., Tindle, A.G., 1984. Trace element dicrimination diagrams for the tectonic interpretation of granitic rocks. J. Petrol. 25, 956–983.

Pearce, J.A., Peate, D.W., 1995. Tectonic implications of the composition of volcanic arc magmas. Annu. Rev. Earth Planet. Sci. 23, 251–285.

Pearce, T.H., Gorman, B.E., Birkett, T.C., 1977. The relationships between major element chemistry and tectonic setting of basic and intermediate volcanic rocks. Earth Planet. Sci. Lett. 36, 121–132.

Philpotts, J.A., Schnetzler, C.C., 1979. Phenocryst-matrix partition coefficients for K, Rb, Sr and Ba, with applications to anorthosite and basalt genesis. Geochim. Cosmochim. Acta 34, 307–322.

Rapp, R., Watson, E., 1995. Dehydration melting of metabasalt at 8 ± 32 kbar: implications for continental growth and crust–mantle recycling. J. Petrol. 36, 891–931.

Rollinson, H., 1996. Using Geochemical Data: Evaluation, Presentation, Interpretation. Longman, Harlow, UK, 352 p.

Tatsumi, Y., 1989. Migration of fluid phases and genesis of basalt magmas in subduction zone. J. Geophys. Res. 94, 4697–4707.

Tatsumi, Y., Hamilton, D.L., Nesbitt, R.W., 1986. Chemical characteristics of fluid phase released from a subducted lithosphere and origin of arc magmas: evidence from HP experiments and natural rocks. J. Volcanol. Geoth. Res. 29, 293–309.

Taylor, S.R., McLennan, S.M., 1985. The Continental Crust: Its Composition and Evolution. Blackwell, Oxford, 321 p.

Wilson, M., 1989. Igneous Petrogenesis, A Global Tectonic Approach. Unwin Hyman, London, 400 p.

Yamamoto, H., Nakamura, E., 2000. Timing of magmatic and metamorphic events in the Jijal complex of the Kohistan arc deduced from Sm–Nd dating of mafic granulites. In: Khan, M.A., Treloar, P.J., Searle, M.P., Jan, M.Q. (Eds.), Tectonics of the Nanga Parbat Syntaxis and the Western Himalaya. Geological Society Special Publication 170, pp. 313–319.